Ain Shams Engineering Journal 12 (2021) 3603–3617

Contents lists available at ScienceDirect

Ain Shams Engineering Journal

journal homepage: www.sciencedirect.com

Civil Engineering

Sustainable use of fly-ash: Use of gene-expression programming (GEP) and multi-expression programming (MEP) for forecasting the compressive strength geopolymer concrete

Hong-Hu Chu [a], Mohsin Ali Khan [b], Muhammad Javed [c], Adeel Zafar [b], M. Ijaz Khan [d,*], Hisham Alabduljabbar [e], Sumaira Qayyum [f]

[a] College of Civil Engineering, Hunan University, Changsha 410082, PR China
[b] Department of Structural Engineering, Military College of Engineering (MCE), National University of Science and Technology (NUST), Islamabad 44000, Pakistan
[c] Department of Civil Engineering, COMSATS University Islamabad, Abbottabad Campus, Abbottabad 22060, Pakistan
[d] Department of Mathematics and Statistics, Riphah International University, I-14, Islamabad 44000, Pakistan
[e] Department of Civil Engineering, College of Engineering in Al-Kharj, Prince Sattam Bin Abdulaziz University, Al-Kharj 11942, Saudi Arabia
[f] Department of Mathematics, Quaid-I-Azam University, 45320, Islamabad 44000, Pakistan

A R T I C L E I N F O

Article history:
Received 7 January 2021
Revised 10 March 2021
Accepted 22 March 2021
Available online 4 May 2021

Keywords:
Artificial intelligence (AI)
Gene expression programming (GEP)
Multi expression programming (MEP)
Fly-ash
Waste material
Geopolymer concrete (GPC)

A B S T R A C T

Annually, the thermal coal industries produce billion tons of fly-ash (FA) as a waste by-product. Which has been proficiently used for the manufacture of FA based geopolymer concrete (FGC). To accelerate the usage of FA in building industry, an innovative machine learning techniques namely gene expression programming (GEP) and multi expression programming (MEP) are employed for forecasting the compressive strength of FGC. The comprehensive database is constructed comprising of 311 compressive strength results. The obtained equations relate the compressive strength of FGC with eight most effective parameters i.e., curing regime (T), time for curing (t) in hours, age of samples (A) in days, percentage of total aggregate by volume (% Ag), molarity of sodium hydroxide (NaOH) solution (M), silica (SiO2) solids percentage in sodium silicate (Na2SiO3) solution (%S), superplasticizer (%P) and extra water (%E_W) as percent FA. The accurateness and predictive capacity of both GEP and MEP model is assessed via statistical checks, external validation criteria suggested by different researcher and then compared with linear regression (LR) and non-linear regression (NLR) models. In comparison with MEP equation, the GEP equation has lesser statistical error and higher correlation coefficient. Also, the GEP equation is short and it would be easy to use in the field. So, the GEP model is further utilized for sensitivity and parametric study. This research will increase the re-usage of hazardous FA in the development of green concrete that would leads to environmental safety and monetarist reliefs.

1. Introduction

Fly ash (FA) is the byproduct produced during the coal production process which is collected via electrostatic or mechanical precipitator [1–4]. Throughout the globe, the thermal coal industry yields about 375 million tons of FA per year, which is dumped into landfills without prior treatment [5]. Also, the disposal cost for each ton of FA ranges from \$20 to \$40 [5]. The discarding million tons of FA without proper treatment may cause serious environmental economic issues in the near future [3]. Also, the FA contains hazardous minerals like ferric oxides, alumina, and silica, which pollutes air, water and soil. Which rises various geo-environmental issues and alarming health situation [6–8]. To sustain the safe environment, an effective and proper waste management of FA is needed [9]. FA is composed of ultrafine particles, which works as a poison when goes in the respiratory system of human being and causes anemia, gastroenteritis, dermatitis, cancer, physiological and hepatic disorder [6,8]. It also contaminates

* Corresponding author.
E-mail address: mikhan@math.qau.edu.pk (M. Ijaz Khan).

Peer review under responsibility of Ain Shams University.

Production and hosting by Elsevier

https://doi.org/10.1016/j.asej.2021.03.018
2090-4479/

the underground and surface water and ultimately creates an alarming condition for the whole aquatic life [6].

In the world, after water, the concrete is the most consumable construction material as the annual production of concrete is 25 billion tons [10]. Which consumes 2.6 billion tons of cement and may rise by 25% in the next 10 years [11]. The production of 1 ton of cement consumes 4GJ of energy, and releases an equivalent amount of CO2 in the atmosphere which is 30% of the global CO2 emission [12,13]. Also, limestone is the key component of cement and an acute deficiency of limestone may arise in the next 5 decades [14]. The production of green concrete is desirable for the safe environment. Thus, the utilization of FA as a supplementary cementitious material for the production of green concrete is the best choice.

In the fly-ash geopolymer concrete (FGC) the cement is partially or fully replaced with FA and thus it's use is on rise for two decades [15–57]. However, the anomalous and inconsistent behavior of FA restrict its wide scale application [58]. The mechanical properties of FGC depend on various factors which includes the initial temperature required in the curing regime (T), time for curing (t) in hours, age of samples (A) in days, percentage of total aggregate by volume (% Ag), molarity of sodium hydroxide (NaOH) solution (M), SiO_2 solids percentage in sodium silicate (Na_2SiO_3) solution (%S), superplasticizer (%P) and extra water (%E_W) as percent FA [15–57]. There is a need for the formulization of compressive strength of FGC. For the development of effective mix design formula and to promote the use of toxic material in construction on a massive scale, the use of soft computing methods is the better selection.

The latest research in the extent of Artificial Intelligence (AI) methods contributed to the formulation of consistent, reliable and accurate models to the problems in structural engineering [59]. The artificial neural network (ANN), genetic algorithm, multi expression programming (MEP), support vector regression (SVR) are AI techniques that works on natural tools [60–81]. In all mentioned AI techniques, the available data is trained to solve the problem. The AI methods like SVR and ANN have the capability to detect the complicated and complex configuration and delivers the generalized pattern. Therefore, it is functional in the vast engineering discipline. In these methods, the extensive hidden neurons need an enormous memory, and thus restrict the development of realistic and practical relation between the inputs and outcome. ANN is widely used in the estimation of mechanical properties of concrete. Gatahun et al. [80] applied ANN approach and predicted the compressive strength of rice husk ash concrete from only 66 experimental datapoints [80], while Mashhadban et al. use it for the prediction of workability of self-compacting concrete [69].

These models replicate the realistic and accurate correlation, but not deliver a practical empirical expression. The complex and complicated architecture of ANN model delays its wide scale adoption [72,82]. Researchers developed the ANN model for punching shear strength of concrete slabs. Because of the complex ANN architecture, it become overfitted when compared with the values projected from design codes. This is attributable to their complex structure [83,84]. The multicollinearity is another problem raised in such models. Similarly, the ANN approach is used to evaluate the elastic modulus of recycled aggregate concrete and compressive strength of silica fume concrete [81]. However, purely a graphical interface was established due to the complication in the proposed relationship [81].

The uniqueness of a genetic programming (GP), is that it discards the former established relation to develop the model. Gene expression programming (GEP) is the extended form of GP that encrypts the small program with the help of fixed length chromosomes [85–89]. GEP also delivers an accurate empirical equation, that can be practically used. It is currently utilized in most of the civil engineering areas as an alternative to other machine learning predictive techniques. Which includes the prediction of compressive strength of rice husk ash concrete, mechanical characteristics of silica fume based light weight concrete, and fresh and hardened properties of self-compacting concrete [90–97].

To tackle the mentioned limitations of other machine learning algorithms, an innovative method known as multi-expression programming (MEP) has also been established. The MEP has a unique feature of encoding the multiple equations (chromosomes) in one program. The best between the selected chromosome, is chosen as the ultimate replication of the problem [98]. In comparison with other evolutionary algorithms, MEP is the upgraded version of GP that has the capacity of processing an accurate result even when the difficulty of target is not known [99]. Unlike other machine learning techniques, MEP not require to specify the form of ultimate equation. In the evolution process of MEP, the mathematical inconsistencies are read and eliminated from the ultimate expression. Also, in MEP the process of decoding is much simple related to other soft computing techniques. Besides, the worthy benefits of MEP in comparison with other evolutionary algorithms, its use in civil engineering field is limited. Alavi et al. utilized MEP for the prediction of soil classification on the basis of soil color, liquid limit, plastic limit, percentage of sand, gavels and fine-grained particles [100]. The authors proposed a non-piecewise model for the estimation of degree of consolidation of soil [101]. Some other studies also use MEP for forecasting the elastic modulus of high strength and normal strength concrete [102]. Furthermore, Arabshahi et al. proposed a design model for the confined concrete column by aramid fiber reinforced polymers [99].

Abundant of experimental researches have been directed to evaluate the compressive strength of FGC [15–57]. But the experimental route is time consuming and costly. So, the establishment of a consistent, reliable and accurate equation is desirable that can relate the compressive strength of FGC with the mix proportion variables. The literature discloses that few GEP empirical equations are available for the approximation of the compressive strength of FGC and no equation is revealed that is built on MEP [32]. However, these models are built via the corresponding experimental outcomes. To meet this research gap, this study uses the GEP and MEP machine learning techniques to provide an accurate expression for the future approximation of compressive strength of FGC. A detailed and extensive database assure the consistency, reliability and accuracy of the developed models for the unseen data. To ensure the generalization of the assembled models their performance is accessed via in-depth statistical, parametric and sensitivity analysis. In the end, the comparison of both GEP and MEP model is checked with linear and non-linear regression expressions.

2. Research methodology

This segment deals with the methodology used to build GEP and MEP based equation for the compressive strength of FGC. The methodology employed in this research would be addressed in more depth followed by a quick review of GEP and MEP.

2.1. Gene expression programming (GEP)

The fixed size strings are used in genetic algorithm (GA). Koza extended GA, and suggested an alternative solution known as genetic programming (GP) [103]. Fig. 1 illustrates the method to develop a computer program through GP approach to solve a problem. The incorporation of a spatial parser structure enables GP an efficient machine learning method. However, Three genetic operators were identified in GP, but just tree crossover is used practically, thus creates an enormous parse trees population [103,104].

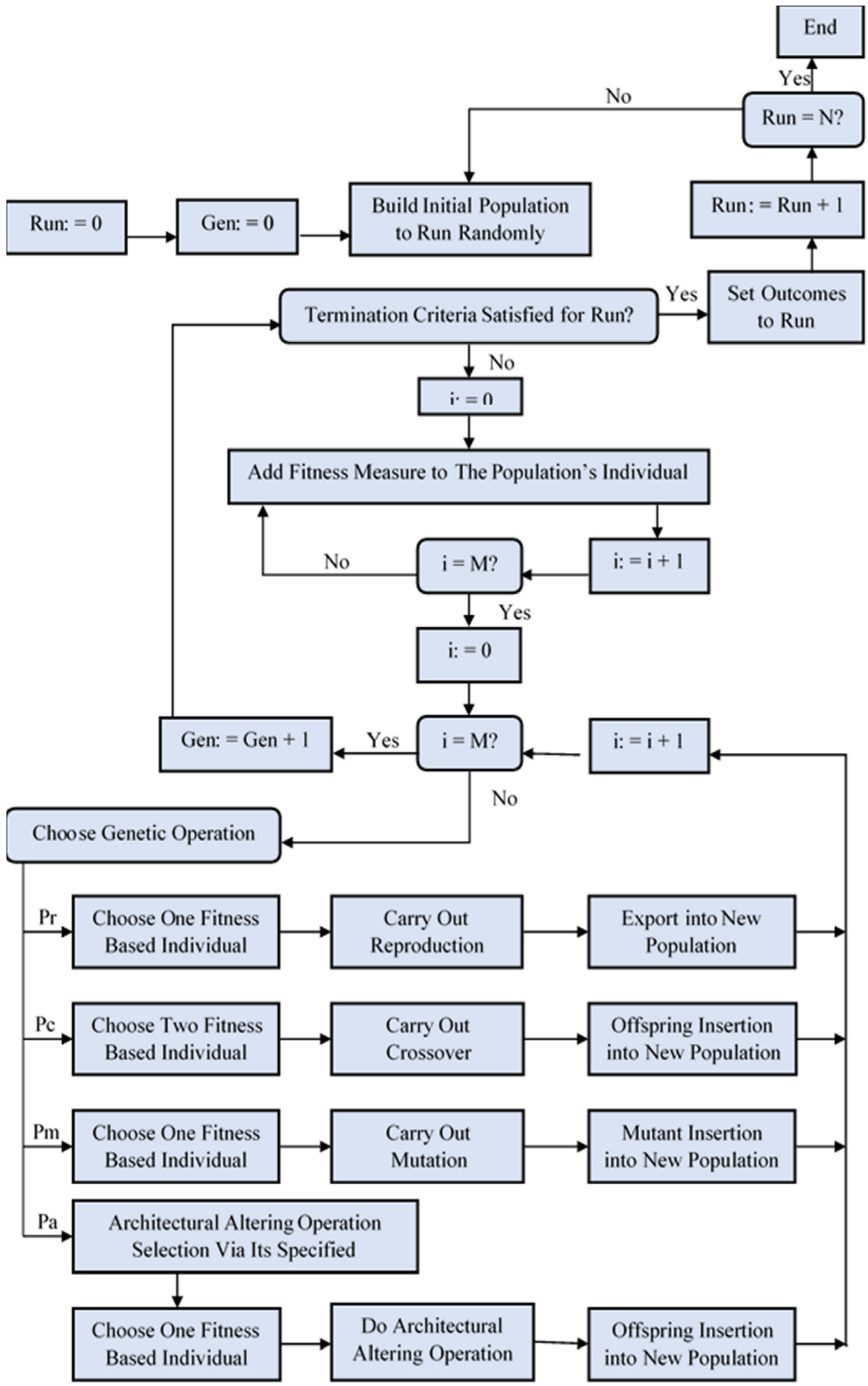

Fig. 1. Flow diagram used by GP algorithm.

One more constraint of GP algorithm is the negligence of neutral genome. Both the phonotype and genotype of the GP algorithm require non-linear configuration, make it impossible to yield popular and easy empirical equation [87]. The GEP approach has been presented by Ferreira as a new variant of the GP approach to reduce its inconsistencies [87]. It combines together the parse trees (GP) and the rudimentary fixed-length linear chromosomes (GA). An important adjustment in GEP is the diffusion of only the genome to the next generation and thus it isn't needed to repeat the whole structure as the entire changes actually occur in a simple linear way. Another notable feature is the creation of model with a single chromosome consisting of different genes, which are then categorized as tail and head [97,105,106]. Every gene of GEP model appears in the shape of a fixed parametric length, a terminating function, and also the mathematical operators. There is also a stabilized link between the terminals and the chromosome in the genetic code operator. The requisite info required to create the GEP model is saved in chromosomes and an innovative language, i.e., karva, has been settled for the inference of such data.

Fig. 2 illustrates the process of the GEP method. It initiates with random creation of fixed span chromosomes for each and every individual. Which are then equal to an expression trees (ET's) and the fitness potential is measured for every individual. For many generations, the repetition extends with novel individuals before the best outcome is achieved.

2.2. Multi expression programming (MEP)

Recently, Oltean recommended another evolutionary algorithm known as multi-expression programming (MEP) [107]. The difference between GEP and MEP algorithm is the consideration of linearity. In MEP, the individuals are considered in variable size units. The outcome of MEP based computation is represented as linear form of string commands which are mix of mathematic operators or terminal variables. The key phases involved in MEP algorithm are illustrated in Fig. 3. The evaluating procedure of MEP method is consisting of: the creation of random chromosome population, use of binary competition process for the choice of two parents and rearranging them by judging the probability of cross-over, recombining the chosen parents for the creation of two off springs, and after mutation of off springs the worst individual in the population is replaced with the strongest one. This cyclic procedure is continuous till the accomplishment of convergence [100,107].

Many research studies utilized the neural network algorithms and GEP method to create an empirical model for the estimation of different properties of ecofriendly concrete. However, the addition of a linear variation makes it easy allowing MEP to differentiate between the phenotype and phenotype of individuals [102]. MEP is highly useful where the uncertainty of targeted equation is unclear, which is the common issue in material engineering problems where a slight difference in the concrete design parameter may have a large effect on concrete strength [107]. In MEP many solutions are coded in one linear chromosome which allows the program to estimate the outcome through searching in wider space.

In comparison with other evolutionary algorithms, the noticeable benefits of GEP and MEP technique would result in the creation of a reliable and accurate models material engineering field. In this study, the GEP and MEP models have been proposed

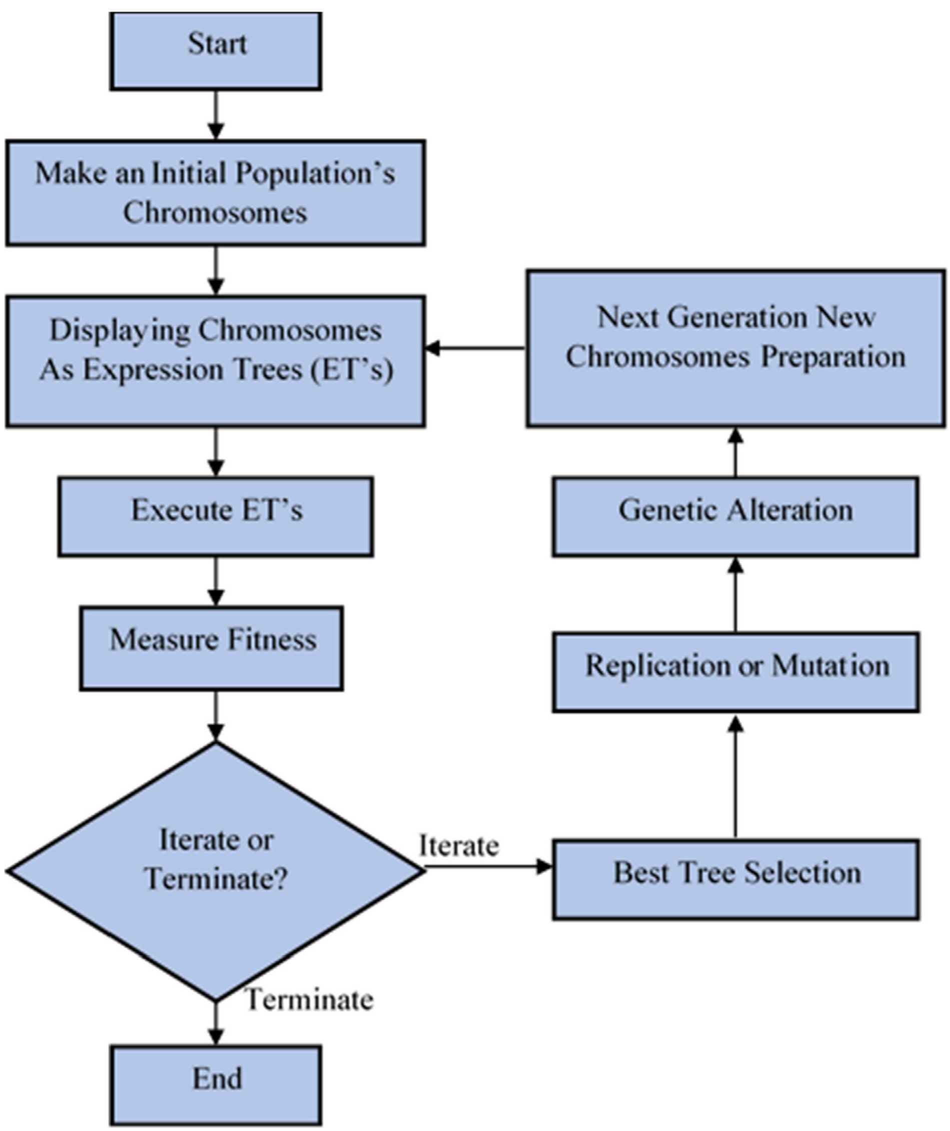

Fig. 2. Flow chart used by GEP algorithm.

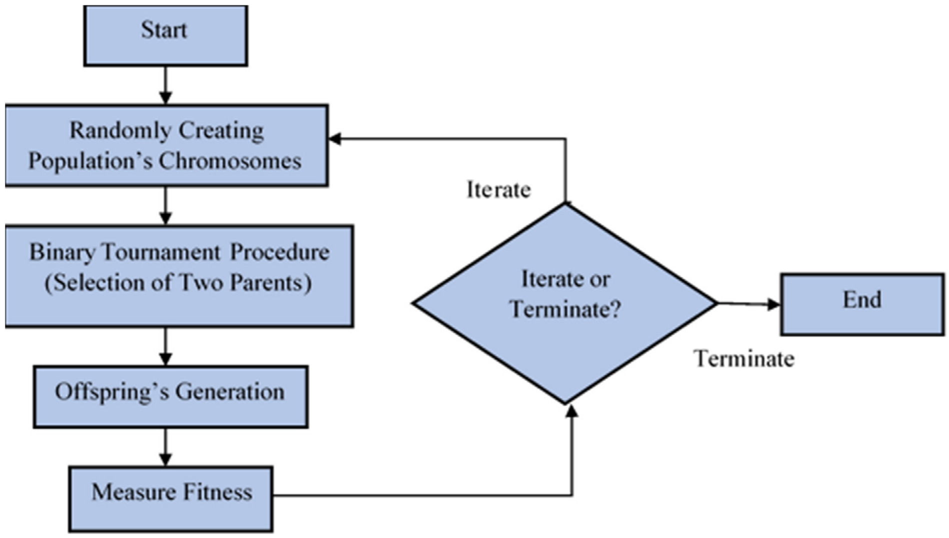

Fig. 3. Flow chart used by MEP algorithm.

for the formulation of compressive strength of FGC. The availability of consistent, accurate and reliable model will help in the use of FA like waste material for construction purposes. This would eventually lead to the resolution of disposal issue connected with FA. Furthermore, it will help in the savage of natural resources and sustainable construction would be promoted.

3. Acquisition of experimental data

The data for the FGC compressive strength (f_c'), was compiled from past research published internationally [15–57]. The whole data base comprises of 311 instances for response f_c' of FGC. In this study the data is collected for two types of specimens i.e., cubic samples (150 mm) and cylindrical samples (100 mm × 200 mm height). The compressive strength relies on the cross-sectional area of the specimens and inversely related to each other. The cube samples have larger cross-sectional area, and will provide higher internal stresses for failure. Thus, the compressive strength of cube samples has been normalized with cylinder specimens by multiplying its compressive strength with a factor of 0.8 [108]. The collected database includes data of input parameter i.e., initial temperature required in the curing regime (T), time for curing (t) in hours, age of samples (A) in days, percentage of total aggregate by volume (% Ag), molarity of sodium hydroxide (NaOH) solution (M), SiO_2 solids percentage in sodium silicate (Na_2SiO_3) solution (%S), superplasticizer (%P) and extra water (%E_W) as percent FA. The accurateness and validity of model be determined by the spreading of the input variables over its range [109]. Fig. 4 shows the input parameter distribution for the model development.

For the more in depth and generalized study, both types of specimen i.e., cylindrical samples and cube samples are count up while developing the database. The output and input variable's range has been given in Table 1. To estimate the compressive strength of FGC accurately, it is recommended to use the established models within the range of input variables given in Table 1.

For the assessment of authenticity, accuracy, and integrity of a database, several trials were performed. The 20% diverged data points from the global rule were excluded in the formation and performance evaluation of the models. An overall of 311 instances were left for the establishment of the GEP and MEP empirical models. This paper divides the 311 instances into two arbitrary sets namely the train (70%) and validation (30%) data set. The training instances helps in the models creation (genetic evolution), While validation instances were utilized to explain the generalization capabilities of the proposed model as indicated in the prior research [59].

4. Models creation and performance assessment criteria

The very first phase in the creation of an accurate artificial intelligence-based model, is the selection of most influential input variables. For this reason, a detailed assessment was conducted and the performance and efficiency of many initial tests were calculated. As a result, the compressive strength of FGC is measured as the function of the Eq. (1).

$$\begin{aligned} Compressive\ \ strength &= f_c'(MPa) \\ &= f(T, t, A, M, A_G, P\%, S\%, E_W\%) \end{aligned} \tag{1}$$

For the creation of generalized and robust GEP and MEP model, several hyper parameters are needed to be defined. The tunning of hyper parameters is based on the trial and error and prior literature references [110]. The progression of the number of programs are identified via size of population. Higher the population size, more complex and accurate model would be created and may consume more time to deliver the best fitted model. However, increasing the population size beyond a certain limit may arise the overfitting problem.

4.1. Creation of GEP model

The population size (chromosomes) defines the run duration of the program. Considering the complexity and difficulty of the model, the chromosomes number are set at 150. The architectural design of GEP model is determined by the number of genes and size of head, which latter determines the complexity of each expression by summation of sub-expression trees (sub-ETs) of the model. Therefore, the head size, number of genes and population size are taken as 10, 3, 150 respectively. Table 2 displays the configured settings of the hyper parameters used for creation of an accurate GEP model. The linking function used for GEP modelling is multiplication along with along other arithmetic operations.

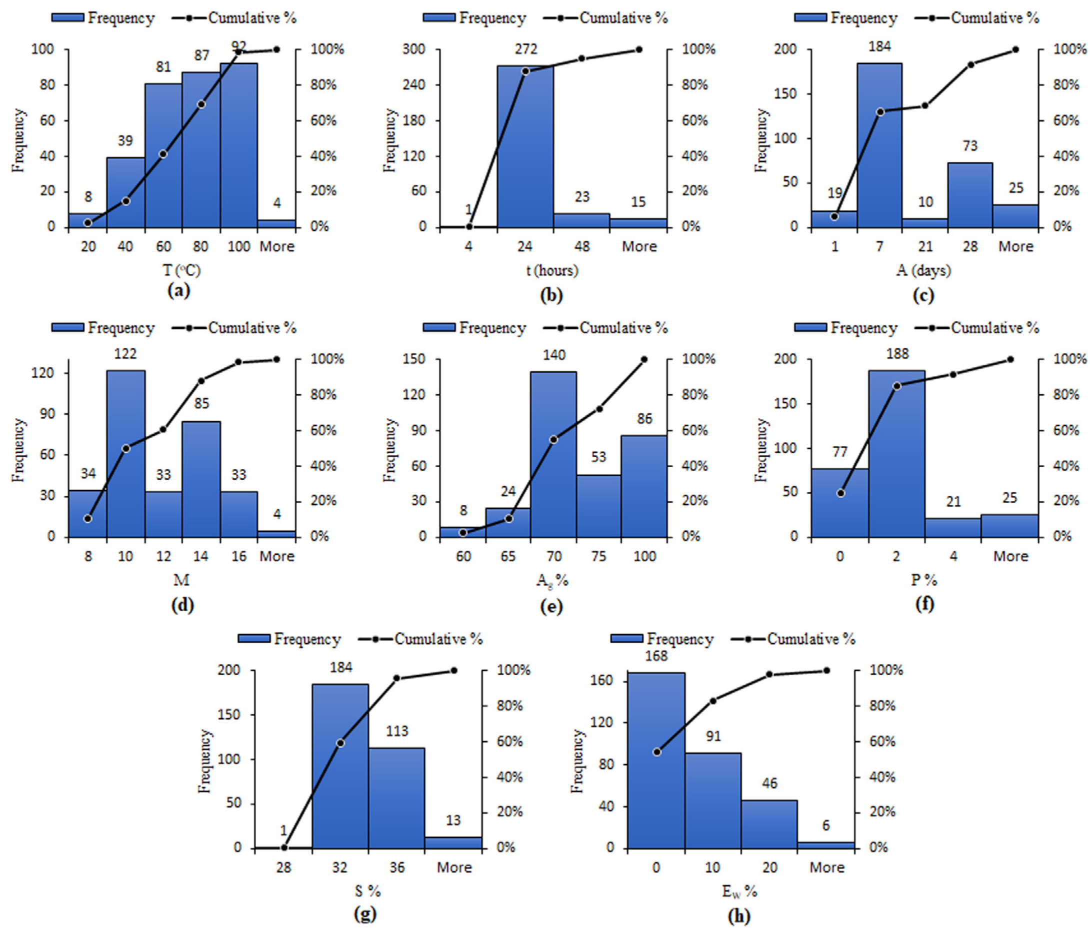

Fig. 4. Frequency distribution histogram of input parameters.

Table 1
Range, average and standard deviation of independent and targeted parameter.

Parameters	Minimum	Maximum	Average	Standard deviation
Independent Variables				
T (°C)	20	120	70.29	25.76
t (hours)	4	96	27.59	13.06
A (days)	1	365	21.57	29.47
M	8	20	11.84	2.66
A_g *(%)*	60	80	72	4.21
P (%)	0	11.3	1.96	2.31
S (%)	27.8	36.7	31.71	2.64
E_W *(%)*	0	35	4.37	5.95
Targeted parameter				
f'_c *(MPa)*	10.5	63	37	10.80

Table 2
GEP model hyper parameter tunning.

GEP algorithm hyper parameters	Settings
Chromosome's number	150
Gene's number	3
Head's size	10
Linkage function	×
Arithmetical operations	−, +, ÷, ×
Constant per gene	10
Data category	Floating
Lower and upper limit	−10 *to* 10
Inversion rate	0.00546
Mutation rate	0.00138
Gene recombination and transposition rate	0.00277
One-point and two-point recombination rate	0.00277

4.2. Creation of MEP model

The MEP modelling was started by taking the sub-population size equal to 10. The chosen hyper parameters used during MEP modelling is presented in Table 3. To create a simple and easy ultimate equation, the basic arithmetical operations were considered i.e., division, subtraction, addition and multiplication. The accuracy of the model to be achieved before termination is defined via number of generations. An executed program that considers higher number of generations would yield results with lesser error. Likewise, the probability of offspring that go through genetic functions, are defined via crossover and mutation rate. The crossover probability range is 50% to 95% [102]. Many sets of combination were tried and the one giving the best results is presented in Table 3.

Table 3
MEP model hyper parameter tunning.

MEP algorithm hyper parameters	Settings
Length of code	40
Sub-population size	250
Sub-population count	50
Arithmetical operations	+, −, ×, ÷
Probability of mutation	0.01
Probability of crossover	0.9
Size of tournament	4
Operators	0.5
Variables	0.5
Generations	1000

It is worth mentioning that the evaluating duration of generation has an effect on the correctness of the proposed model. The evolution of the model is continued indefinitely because of the inclusion of new variables in the system. However, this study considers the stopping criteria for the evolution of model as 2000 generations or the time when less than 0.1% change in fitness function occur.

4.3. Criteria for evaluating performance of MEP and GEP model

A sample coefficient of correlation represented as R is widely being used for the measurement of the effectiveness and efficiency of the model. Due to the insensitivity of R for basic arithmetic's (division and multiplication) of outputs into constant, its mere use for studying the accuracy of the model is highly resisted [111]. Therefore, this study also considers other statistical measures like the RSE: relative square error; RMSE: root mean squared error; MAE: mean absolute error and RRMSE: relative root means square error. For more in-depth assessment of the model performance, the use performance index represented as (ρ) is highly encouraged. It plays the role of both functions i.e., RRMSE and R. [109]. The expressions for the stated error functions are presented as Eqs. (2)–(7).

$$RMSE = \sqrt{\frac{\sum_{j=1}^{n}(e_i - o_i)^2}{n}} \tag{2}$$

$$MAE = \frac{\sum_{j=1}^{n}|e_i - o_i|}{n} \tag{3}$$

$$RSE = \frac{\sum_{j=1}^{n}(o_i - e_i)^2}{\sum_{j=1}^{n}(\bar{e} - e_i)^2} \tag{4}$$

$$RRMSE = \frac{1}{|\bar{e}|}\sqrt{\frac{\sum_{j=1}^{n}(e_i - o_i)^2}{n}} \tag{5}$$

$$R = \frac{\sum_{j=1}^{n}(e_i - \bar{e}_i)(o_i - \bar{o}_i)}{\sqrt{\sum_{j=1}^{n}(e_i - \bar{e}_i)^2 \sum_{i=1}^{n}(o_i - \bar{o}_i)^2}} \tag{6}$$

$$\rho = \frac{RRMSE}{(1+R)} \tag{7}$$

In the stated statistical measure equations,$\bar{e}_i$, and $\bar{o}_i$ symbolizes the mean experimental value and mean models' outcome respectively. While e_i and o_i denotes the j^{th} experimental instance and models outcome respectively. The count of total instances is denoted by n. For the effective and reliable machine learning model, it is compulsory to have higher value of R and lower statistical error values such as RRMSE, MAE, RSE, RMSE, and ρ. The previous studies recommended that R must be higher than 0.8 for the best calibrated model and ρ nearer equal to 0 [112,113].

5. Results and discussion

5.1. Formulization of fc' via GEP technique

Fig. 5 illustrates the expression trees (ETs) delivered by GeneXproTool, which is decoded to get an empirical expression for the prediction of compressive strength of FGC. It uses only the four rudimentary arithmetical operators i.e., −, ÷, +, ×. Eq. (9) is the simple expression extracted from these expression trees. Which is composed of four different variables A (extracted from Sub-ET 1), B (extracted from Sub-ET 2), and C (extracted from Sub-ET 3). The description of different symbols used in the expression trees is presented in Table 4.

Eq. (9) is the simple, easy and practicable equation which can be accessible to predict f_c' of FGC.

$$f_c'(MPa) = A \times B \times C \tag{9}$$

where;

$$A = 4.1 - \frac{18.46}{8.94 + P\%} \times \frac{S\% + E_W\%}{A_g - S\%} \tag{10}$$

$$B = 1 + \frac{(2 \times A) - 131.23}{T \times t} \tag{11}$$

$$C = \frac{T - (2 \times M)}{9} - \frac{2}{M - 9} + 11.91 \tag{12}$$

Fig. 6 is constructed to compare the regression lines of compressive strength of model predicted outcome and experimental values of both training and validation set. It can be clearly seen that regression lines' slope for the validation instances is equals to 1.0013 and that for training instances is 0.9726. The inclination of regression lines is almost analogous and quite near to the ideal fit (equals to 1).

5.2. Formulization of fc' via MEP technique

The MEP outcome is decoded to achieve an empirical expression for the estimation of compressive strength of FGC that encompass the effect of eight independent variables considered in this study. The ultimate mathematical equations delivered via MEP are presented as Eq. (13).

$$f_c'(MPa) = \left(\frac{(a') \times \left(e + \frac{g}{a'}\right) - \left(\frac{c'}{b'}\right)}{g}\right) - \left(\frac{h}{b'}\right) - \left(\frac{f^2}{b}\right) - \left(\frac{\left(2 \times \left(d - c - b + g + f^2 + \left(\frac{c'}{b'}\right)\right)\right)}{b}\right) \tag{13}$$

where; $a = T; b = t; c = A; d = M; e = A_g; f = \%P; g = \%S; h = \%E_W$

And $a' = f + 2\sqrt{a}; b' = f + \sqrt{a}; c' = h\sqrt{a}$

For both stages i.e., training stage and validation stage, the experimental and MEP predicted output is compared in Fig. 7. On this graph, the regressions line equation is also presented. For an ideal scenario, the inclination of the regression line must be near to 1. The Fig. 7 inferred that the regression line inclination for training instances and validation instances comes out to be 0.9626 and 1.0078 respectively. These values are almost close to each other and nearer to 1. Which dictates that the model is trained well and holds a greater generalization ability, replicating that the model would also perform good on the unseen and fresh

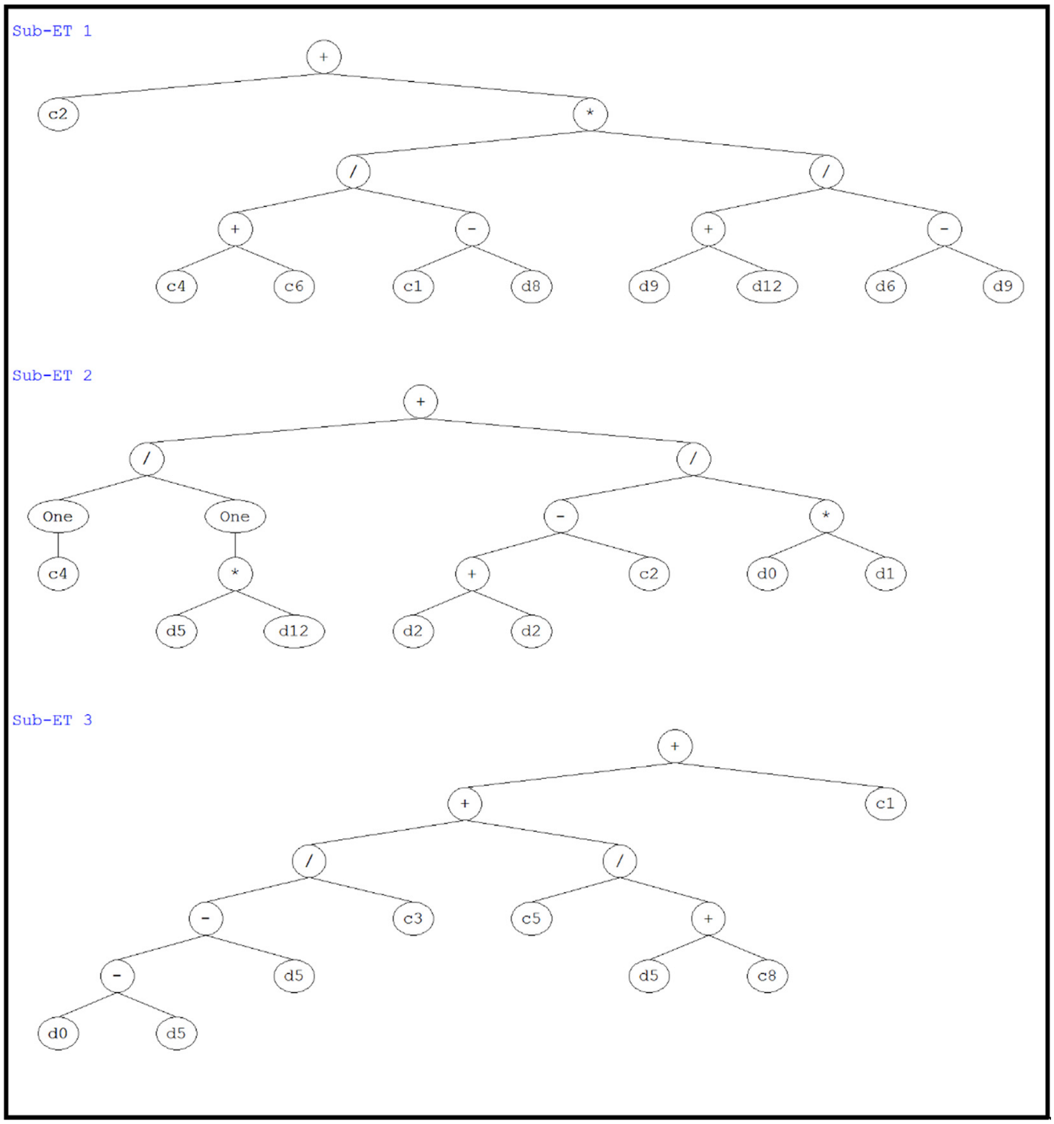

Fig. 5. The expression trees for the extraction of GEP equation.

Table 4
Explanation of the expression tree indicators.

Independent variable	Expression tree indicator	Description
T (°C)	d_0	Initial temperature required in the curing regime
t (hours)	d_1	Time required for curing of samples
A (days)	d_2	Age of samples
M	d_5	Molarity of sodium hydroxide (NaOH) solution
Ag	d_6	Percentage of total aggregate by volume
P (%)	d_8	Superplasticizer as percent fly ash
S (%)	d_9	SiO_2 solids percentage in sodium silicate (Na_2SiO_3) solution
Ew (%)	d_{12}	Addition of extra water as percent fly ash

data. However, in comparison with GEP model, the slope of regression lines dictates that MEP model stands at second.

5.3. Statistical errors assessment of GEP model

The literature recommended that for the creation of an accurate GEP model, the minimum ratio limit between the database points to the independent variables must be three and for an ideal case that must surpasses 5, while this study uses higher value which is 38 [109]. Table 5 and Table 6 denotes the statistical error analysis of the proposed GEP equation for both the train instances and validation instances. The results signify the accurateness and strong correlation between the projected outcome of GEP equation and experimental results. For the GEP equation, in the training phase, the values of statistical errors like RSE, R, MAE and RMSE are 0.253, 0.8648, 5.624 and 5.901 respectively. While in the validation phase these values are 0.0315, 0.9844, 1.319 and 1.521 respectively. The stated error values for both in training phase and validation phase are analogous, which directs that the projected GEP expression is accurate and generalized and can be used for the fresh data. Table 6 shows that the performance index reaches to 0, while for an ideal case it must be equal to 0.

The plot between the absolute error of proposed GEP equation and experimental values is shown in Fig. 8, which gives an overview of the overall maximum percentage of error in GEP model. The maximum error i.e., 8.8 MPa and average error i.e., 4.2 MPa, validates that the experimental results and GEP equation results are almost similar. It is important to mention that the frequencies of maximum values of error is much lesser. For 90% instances,

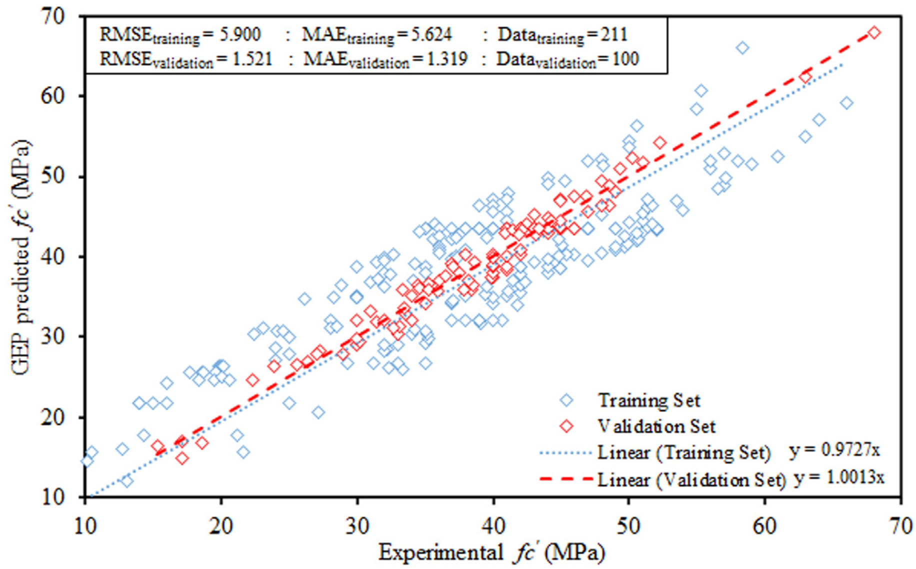

Fig. 6. Assessment of GEP predicted f_c' and experimental values.

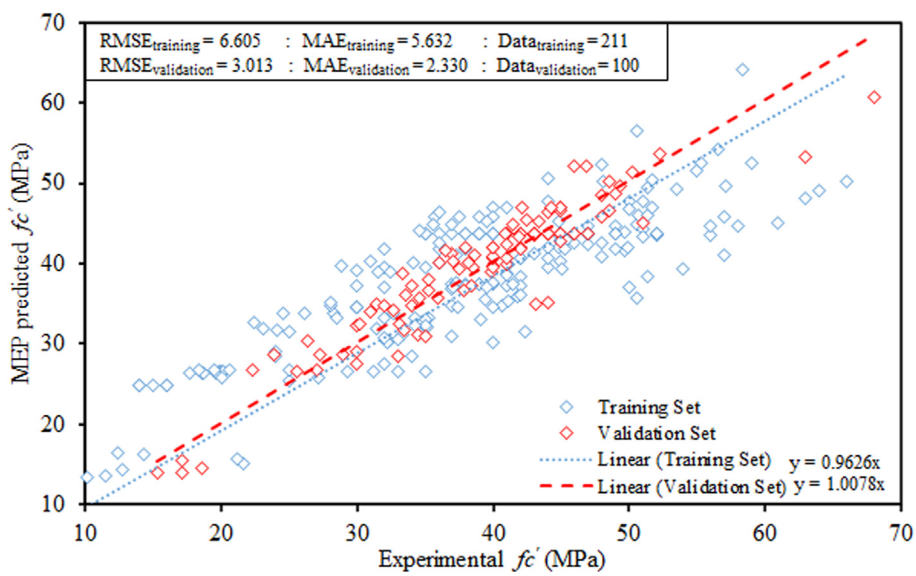

Fig. 7. Assessment of MEP predicted f_c' and experimental values.

Table 5
Checking of statistical error of GEP and GEP equations.

Model	MAE		RMSE		RSE	
	Training	Validation	Training	Validation	Training	Validation
GEP	5.624	1.319	5.901	1.521	0.2532	0.0315
MEP	5.632	2.330	6.605	3.013	0.3173	0.1236

Table 6
Validation of GEP and MEP equation using Performance index.

Model	R		RRMSE (%)		ρ	
	Training	Validation	Training	Validation	Training	Validation
GEP	0.8648	0.9844	15.495	3.895	0.0831	0.0196
MEP	0.8314	0.9386	17.345	7.713	0.0947	0.0397

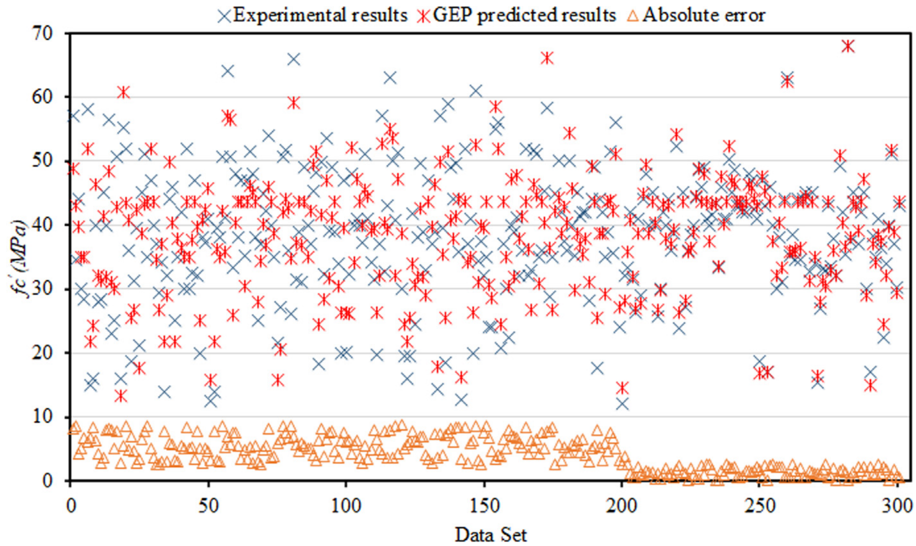

Fig. 8. Representation of absolute error of GEP predicted and experimental results.

absolute maximum error and percent average error of the whole data is lesser than 7% and 4% respectively. Which confirms the generalized nature of GEP model.

5.4. Statistical errors assessment of MEP model

As discussed earlier, the efficiency of any machine learning model depends on the values of statistical indicators i.e., MAE, RMSE, R, and RSE. For both the training and validation instances, the value of such indicators is presented in Table 5 and Table 6. Which depicts that a high correlation exists between the MEP predicted outcomes and experimental results. Table 6 illustrates that for MEP model the R value in the training and validation stage is equals to 0.8314 and 0.9386 respectively. While the RMSE, RSE and MAE in the training phase are 6.605, 0.317, and 5.632 respectively and in the validation phase these values comes out to be 3.013, 0.1236, and 2.330 respectively. In each phase, the values of statistical indicators are much lower and closer to each other. Table 6 depicts that the performance index for MEP model also approaches to 0, dictating the generalization of the model.

To study the broader picture of the model, the plot of absolute error of MEP model is shown in Fig. 9. Which shows that for the whole data set the mean and maximum error of MEP predictive results is MPa and MPa. It is worthy to state that the occurrence of maximum error of MEP predicted result is lower, but greater than GEP model. Thus, it can be concluded that for 90% instances, absolute maximum error and percent mean error of the whole data is lesser than 14% and 9% respectively. Which confirms the generalized nature of GEP model. Both the MEP and GEP models have high predictive capacity. However, the GEP equation has lesser statistical error and higher correlation coefficient. Also, the GEP equation is short and it would be easy to use in the field.

5.5. External validation of MEP and GEP models

Both the GEP and MEP equation are subjected to external testing criteria recommended by previous papers. The review of these external validation checks is presented in Table 7. The (S' *or* s) replicates the inclination of the regression lines passing over the origin. Their values must approach to 1. [98]. As displayed in

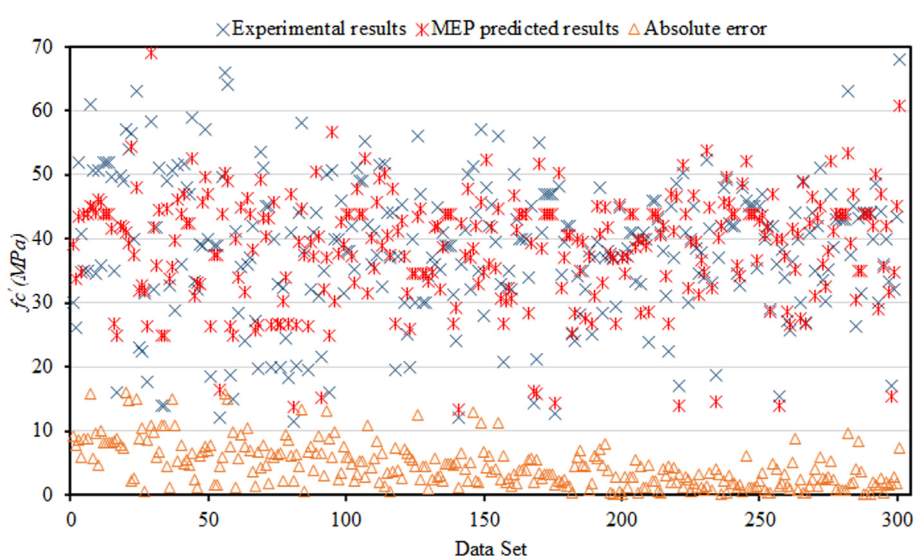

Fig. 9. Representation of absolute error of MEP predicted and experimental results.

Table 7
Validating the GEP and MEP equations via the criteria suggested in literature.

Suggested expression	Condition	GEP equation	MEP equation
$s = \frac{\sum_{i=1}^{n}(e_i \times m_i)}{\sum_{i=1}^{n}(e_i^2)}$	$0.85 < s < 1.15$	1.001	1.007
$s' = \frac{\sum_{i=1}^{n}(e_i \times m_i)}{\sum_{i=1}^{n}(m_i^2)}$	$0.85 < s' < 1.15$	0.9973	0.9867
$R_o^2 = 1 - \frac{\sum_{i=1}^{n}(m_i - e_i^o)^2}{\sum_{i=1}^{n}(m_i - \bar{m}_i^o)^2}, e_i^o = s \times m_i$	$R_o^2 \cong 1$	0.9999	0.9984
$R_o'^2 = 1 - \frac{\sum_{i=1}^{n}(e_i - m_i^o)^2}{\sum_{i=1}^{n}(e_i - \bar{e}_i^o)^2}, m_i^o = s' \times e_i$	$R_o'^2 \cong 1$	0.9659	0.8701

Table 7, both the GEP and MEP equation are highly accurate and satisfies the stated criteria. Another paper recommended the check of $R_o'^2$ and R_o^2. Their presence replicates the square coefficient of correlation between the proposed model results and experimental results or experimental results and proposed model results respectively. Their values also must approach to 1 [100]. Table 7 displays that, for both the GEP and MEP equation, these checks are also fall in the required limit. Thus, the presented GEP and MEP equation are reliable and accurate and have the capacity to predict the compressive strength of FGC.

5.6. Comparison between predicted values of GEP, MEP, linear and non-linear regression models

This study considered eight different independent variables for forecasting the compressive strength of FGC via MEP and GEP algorithms. To data, no equation is available for forecasting the compressive strength of FGC. that considered the same independent variables. So, it is obligatory to compare the developed MEP and GEP ultimate results with the results of non-linear regression (NLR) and linear regression (LR) expressions developed for the same independent parameters.

The predicted results for compressive strength of FGC by GEP and MEP expression are plotted against experimental values in Fig. 10. While Fig. 11 illustrates the comparison of GEP predicted output with LR and NLR. The LR and NLR expression for forecasting the compressive strength of FGC are presented as Eqs. (14) and (15).

$$f'_c = 31.1 + 0.294T + 0.157t + 0.0676A - 1.103M + 0.653A_G\% + 1.72P\% - 1.69S\% - 0.597E_W\% \quad (14)$$

$$f'_c = 23.95 + 5.1(T)^{0.48} + 5.69(t)^{0.29} + 1.81(A)^{0.428} - 14.95(M)^{0.406} + 0.48(A_G\%)^{0.961} + 5.43(P\%)^{0.486} - 0.128(S\%)^{1.648} - 0.00189(E_W\%)^{2.871} \quad (15)$$

The lowest values of RMSE and ρ have been observed for GEP model as compared to MEP, LR and NLR predictive models. The RMSEtraining of GEP model is 11%, 15%, and 6% lower than MEP, LR and NLR models respectively and $\rho_{training}$ is 13%, 17%, and 7% lower respectively. In the validation phase, the GEP model provides an outburst performance i.e., $\rho_{validation}$of GEP model is 51%, 62%, 55% better than MEP, LR, and NLR models respectively. Moreover, Fig. 11 dictates that LR and NLR models collapsed in covering the higher range compressive strength effectively that obstructs the utilization of regression models for practical use.

The suggested GEP equation perform well than MEP, LR and NLR equations, in both training and validation phase. Also, the MEP equation is impractical and lengthy. Furthermore, the regression model carries some disadvantages. It assumes the pre-defined equations and the normality of residuals for prediction purpose [112]. While GEP model accurately encompass the non-linearity between the explanatory variables and response parameter, giving lesser error as compared to MEP, LR and NLR equations.

5.7. Sensitivity and parametric analysis via GEP equation

As GEP equation (see Eq. (9)) is simple and easy and perform better than MEP equation, so sensitivity analysis (SA) of GEP equation is accomplished for investigating the relative influence of the input parameters utilized for the f'_c of FGC, using Eq. (16) and (17).

$$N_i = f_{max}(x_i) - f_{min}(x_i) \quad (16)$$

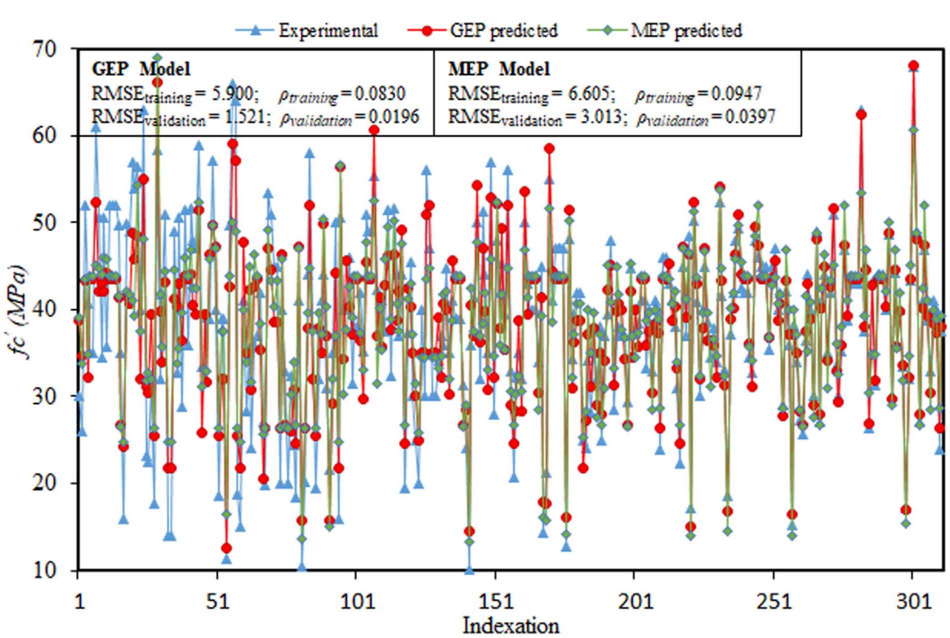

Fig. 10. Comparison between predicted results via MEP and GEP model.

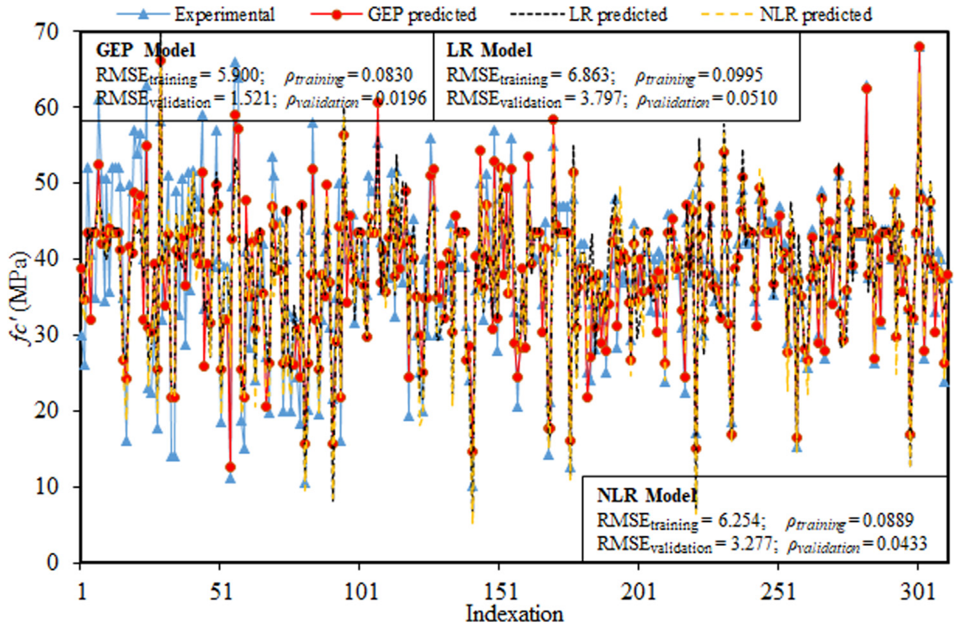

Fig. 11. Comparison between predicted results via GEP, LR and NLR model.

$$SA = \frac{N_l}{\sum_{n}^{j=1} N_j} \tag{17}$$

where maximum and minimum of the predictive outcome relied on its input dominion, denoted by $f_{max}(x_i)$ and $f_{min}(x_i)$ respectively. while rest of the input parameters are held at an average value. Results for sensitivity analysis for compressive strength is presented in Fig. 12. Which make clear that, from a material engineering perception, the input factors contribution to the f'_c of FGC is fairly similar.

In addition, the usefulness of utmost prominent dependent parameters in the f'_c FGC's estimation is achieved by doing parametric study of GEP expression. Alteration is detected in f'_c of FGC by altering the value of the only one dependent variable between minimum and maximum value and rest all other dependent variables was held at average values. The ultimate results of GEP model's parametric study are illustrated in Fig. 13.

Curing temperature is considered to be the most stimulating parameter for the regulating the f'_c of FGC as depicted in Fig. 12. An increase in curing temperature till 120^0 may result in the increase of f'_c of FGC, and vice versa as mentioned in the literature [15,16,20,26,30,42,55]. It has also been seen that the response parameter i.e., f'_c rises linearly with increase in temperature required for curing of the specimens.

The f'_c increases with the elongation of curing time till 96 h Various researchers observed the similar trend [15,16]. However, the rate of increment beyond 24 h get reduced as depicted in the curve in Fig. 13. [20]. The flatness and then decrease in curve beyond 96 h can be clarified via the truth that geo-polymerization is a quick process. Similar results are also reported in the previous studies [35,52].

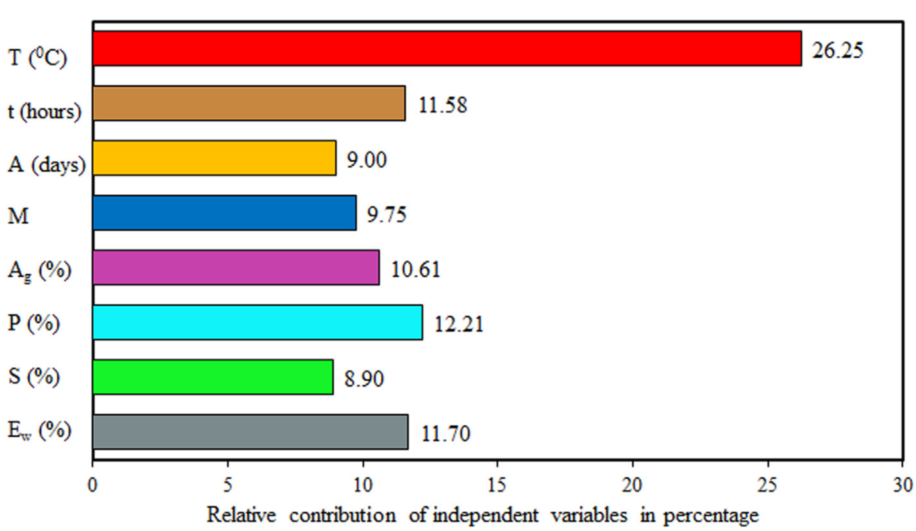

Fig. 12. Relative contribution of independent variables in percentage.

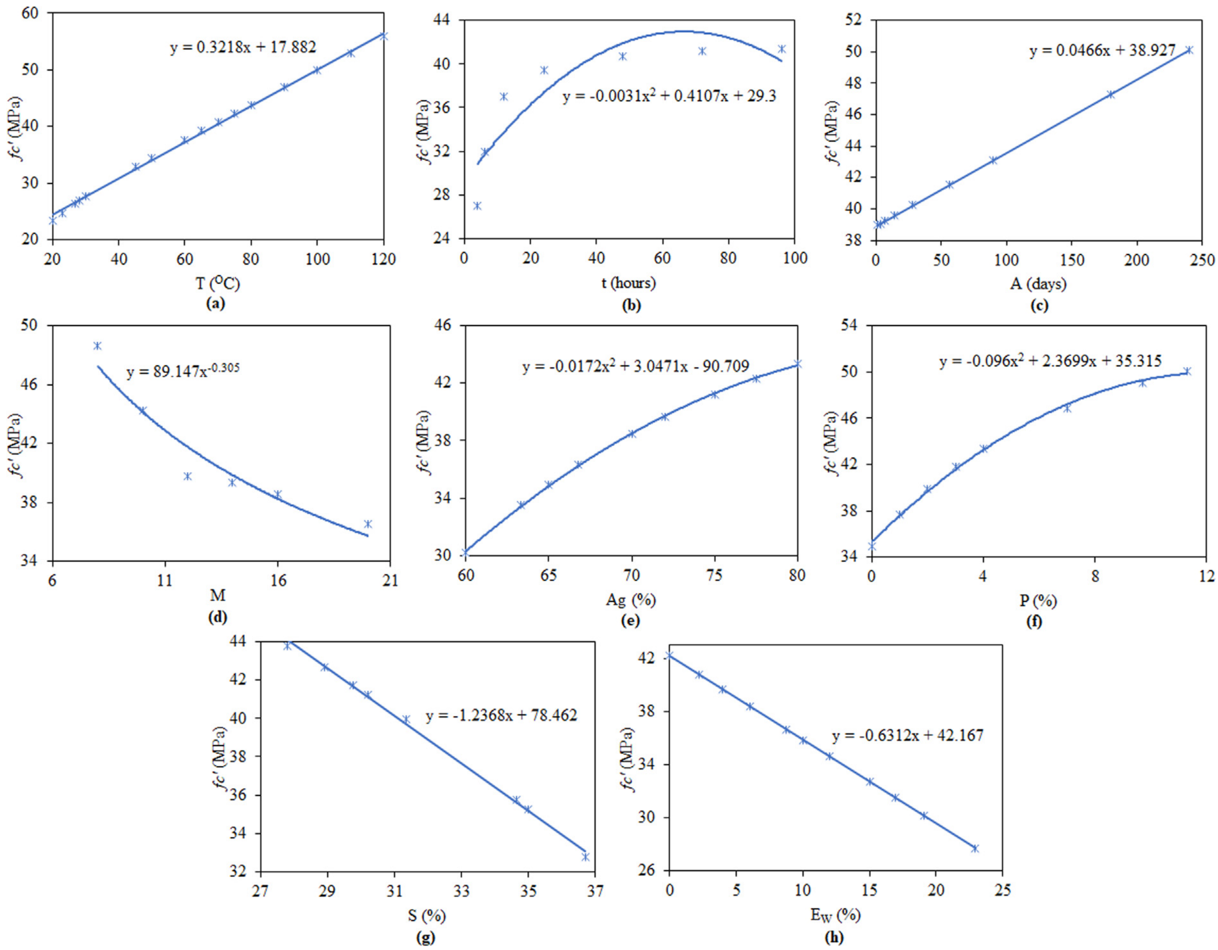

Fig. 13. Variation of compressive strength of FGC by varying the independent variables.

To achieve a workable FGC, the incorporation of plasticizer or the addition of extra water is estimated [16,55,114]. The use of plasticizer or the addition of extra water comparatively contributes 12.1% and 11.7% respectively. The FGC's compressive strength go down with the inclusion of extra water and rises by adding super plasticizers as seen in Fig. 13. The segregation and bleeding in the fresh FGC may be caused by adding the extra water beyond a specific limit.

In short, Fig. 13 shows the same results as conducted by different researchers in the past [15,20,30,42,55]. Thus, the results of parametric study via proposed GEP based empirical equation for forecasting the *fc'* of FGC, accurately encompass the impact of all the independent variables considered.

6. Conclusion

Every year, the coal industry produces billion tons of fly-ash (FA) as a waste by-product. To reduce its harmful impact on the environment it has been proficiently used by different researchers for the production of FA based geopolymer concrete (FGC). This research is focused on accelerating the utilization of FA in building industry. An innovative machine learning techniques namely gene expression programming (GEP) and multi expression programming (MEP) were employed for forecasting the compressive strength of FGC. The comprehensive database is constructed from the published researches, which is comprised of 311 compressive strength results of FGC. The GEP and MEP equations are obtained that relates the compressive strength of FGC with eight most effective parameters i.e., curing regime (T), time for curing (t) in hours, age of samples (A) in days, percentage of total aggregate by volume (% Ag), molarity of sodium hydroxide (NaOH) solution (M), silica (SiO_2) solids percentage in sodium silicate (Na_2SiO_3) solution (% S), superplasticizer (%P) and extra water (%E_W) as percent FA. The accurateness and predictive capacity of both the GEP and MEP model is assessed via statistical checks (R, RMSE, MAE, RSE, RRMSE and ρ) and then suggested models are subjected to external validation criteria suggested by different researcher. The models are also compared with linear regression (LR) and non-linear regression (NLR) equations. Both the models correctly satisfy the validation criterion and reveals that both the artificial intelligence-based models have higher generalization capacity and can be used for the unseen and fresh data. In comparison with MEP equation, the GEP equation has minimal statistical error and higher correlation coefficient. Also, the GEP equation is short and simple and it would be better to use in the field. In last the GEP model is further utilized for sensitivity and parametric study. Which confirms that GEP model accurately covers the impact of each independent parameter. This research will increase the re-usage of hazardous FA in the development of green concrete that would leads to environmental safety and monetarist reliefs. Instead of disposing FA into landfill, its use in concrete would also reduce the cost of construction.

Author contribution

All the authors contribute equally in the execution of this research.

Declaration of Competing Interest

All the authors declare no conflict of interest.

Acknowledgement

We are thankful to the National University of Science and Technology (NUST), Islamabad for helping in initiating this research work.

References

[1] Aprianti E. A huge number of artificial waste material can be supplementary cementitious material (SCM) for concrete production–a review part II. J Cleaner Prod 2017;142:4178–94.
[2] Ibrahim HA, Razak HA. Effect of palm oil clinker incorporation on properties of pervious concrete. Constr Build Mater 2016;115:70–7.
[3] Akmal AMN et al. Utilization of fly ash as partial sand replacement in oil palm shell lightweight aggregate concrete. IOP Conf. Series: Materials Science and Engineering, 2017.
[4] Rafieizonooz M et al. Investigation of coal bottom ash and fly ash in concrete as replacement for sand and cement. Constr Build Mater 2016;116:15–24.
[5] Bayar T. Best practices for managing power plant coal ash. 2015 Mar, 18; Available from: https://www.powerengineeringint.com/coal-fired/managing-coal-ash/.
[6] Ghosh K, Mukherjee K, Saha S. Fly ash of thermal power plants: review of the problems and management options with special reference to the Bakreshwar thermal power plant, Eastern India. Int J Geol Earth Environ Sci 2015;5(2):74–91.
[7] Nadesan MS, Dinakar P. Mix design and properties of fly ash waste lightweight aggregates in structural lightweight concrete. Case Stud Constr Mater 2017;7:336–47.
[8] Tiwari MK, Bajpai S, Dewangan UK. Fly ash utilization: A brief review in Indian context. Int Res J Eng Technol (IRJET) 2016;3(4):2395–10056.
[9] Nordin N et al. Utilization of Fly ash waste as construction material. Int J Conservat Sci 2016;7(1).
[10] Watts J. Concrete: the most destructive material on Earth. 2020; Available from: https://www.theguardian.com/cities/2019/feb/25/concrete-the-most-destructive-material-on-earth.
[11] Aleem MA, Arumairaj P. Geopolymer concrete–a review. Int J Eng Sci Emerg Technol 2012;1(2):118–22.
[12] Das SK, et al., Incorporation of Ultrafine Rice Husk Ash (URHA) in Geopolymer Concrete. 2019.
[13] Li H et al. Assessing the life cycle CO2 emissions of reinforced concrete structures: Four cases from China. J Cleaner Prod 2019;210:1496–506.
[14] Kumar BS, Sen A, Seshu DR. Shear strength of fly ash and GGBS based geopolymer concrete. In: Advances in Sustainable Construction Materials. Springer. p. 105–17.
[15] Joseph B, Mathew G. Behavior of geopolymer concrete exposed to elevated temperatures. Cochin University of Science And Technology; 2015.
[16] Ahmed MF, Nuruddin MF, Shafiq N. Compressive strength and workability characteristics of low-calcium fly ash-based self-compacting geopolymer concrete. Int J Civil Environ Eng 2011;5(2):64–70.
[17] Deb P, Nath P, Sarker P. Properties of fly ash and slag blended geopolymer concrete cured at ambient temperature. New Develop Struct Eng Construct 2013:571–6.
[18] Deb P, Nath P, Sarker P. Sulphate resistance of slag blended fly ash based geopolymer concrete. In: Concrete 2013: Proceedings of the 26th Biennial National Conference of the Concrete Institute of Australia. Concrete Institute of Australia, 2013.
[19] Partha SD, Pradip N, Prabir KS. Strength and permeation properties of slag blended fly ash based geopolymer concrete. Advanced Materials Research. Trans Tech Publ; 2013.
[20] Hardjito D, Rangan BV. Development and properties of low-calcium fly ash-based geopolymer concrete. Dissertation 2005.
[21] Galvin B, Lloyd N. Fly ash based geopolymer concrete with recycled concrete aggregate. In: Proceedings of the CONCRETE 2011 Conference. The Concrete Institute of Australia, 2011.
[22] Kusbiantoro A et al. The effect of microwave incinerated rice husk ash on the compressive and bond strength of fly ash based geopolymer concrete. Constr Build Mater 2012;36:695–703.
[23] Lloyd N, Rangan V. Geopolymer concrete with fly ash. In: Proceedings of the Second International Conference on sustainable construction Materials and Technologies. UWM Center for By-Products Utilization, 2010.
[24] Nuruddin MF et al. Utilisation of waste material in geopolymeric concrete. Proc Inst Civil Eng-Construct Mater 2011;164(6):315–27.
[25] Nath P, Sarker PK. Flexural strength and elastic modulus of ambient-cured blended low-calcium fly ash geopolymer concrete. Constr Build Mater 2017;130:22–31.
[26] Olivia M, Nikraz H. Properties of fly ash geopolymer concrete designed by Taguchi method. Mater Des (1980-2015) 2012;36:191–8.
[27] Sarker PK, Haque R, Ramgolam KV. Fracture behaviour of heat cured fly ash based geopolymer concrete. Mater Des 2013;44:580–6.
[28] Shi X et al. Mechanical properties and microstructure analysis of fly ash geopolymeric recycled concrete. J Hazard Mater 2012;237:20–9.
[29] Sujatha T, Kannapiran K, Nagan S. Strength assessment of heat cured geopolymer concrete slender column. 2012.
[30] Vora PR, Dave UV. Parametric studies on compressive strength of geopolymer concrete. Procedia Eng 2013;51:210–9.
[31] Wardhono A et al. Comparison of long term performance between alkali activated slag and fly ash geopolymer concretes. Constr Build Mater 2017;143:272–9.
[32] Lokuge W et al. Design of fly ash geopolymer concrete mix proportions using Multivariate Adaptive Regression Spline model. Constr Build Mater 2018;166:472–81.
[33] Mehta A, Siddique R. Properties of low-calcium fly ash based geopolymer concrete incorporating OPC as partial replacement of fly ash. Constr Build Mater 2017;150:792–807.
[34] Mehta A, Siddique R. Sulfuric acid resistance of fly ash based geopolymer concrete. Constr Build Mater 2017;146:136–43.
[35] Ramujee K, PothaRaju M. Mechanical properties of geopolymer concrete composites. Mater Today: Proc 2017;4(2):2937–45.
[36] Sathanandam T et al. Low carbon building: Experimental insight on the use of fly ash and glass fibre for making geopolymer concrete. Sustainable Environ Res 2017;27(3):146–53.
[37] Pasupathy K et al. Durability of low-calcium fly ash based geopolymer concrete culvert in a saline environment. Cem Concr Res 2017;100:297–310.
[38] Nuaklong P, Sata V, Chindaprasirt P. Influence of recycled aggregate on fly ash geopolymer concrete properties. J Cleaner Prod 2016;112:2300–7.
[39] Wongsa A et al. Properties of lightweight fly ash geopolymer concrete containing bottom ash as aggregates. Constr Build Mater 2016;111:637–43.
[40] Shaikh FUA. Mechanical and durability properties of fly ash geopolymer concrete containing recycled coarse aggregates. Int J Sustainable Built Environ 2016;5(2):277–87.
[41] Shehab HK, Eisa AS, Wahba AM. Mechanical properties of fly ash based geopolymer concrete with full and partial cement replacement. Constr Build Mater 2016;126:560–5.
[42] Aliabdo AA, Abd Elmoaty M, Salem HA. Effect of cement addition, solution resting time and curing characteristics on fly ash based geopolymer concrete performance. Constr Build Mater 2016;123:581–93.
[43] Okoye F, Durgaprasad J, Singh N. Mechanical properties of alkali activated flyash/Kaolin based geopolymer concrete. Constr Build Mater 2015;98:685–91.
[44] Ganesan N, Abraham R, Raj SD. Durability characteristics of steel fibre reinforced geopolymer concrete. Constr Build Mater 2015;93:471–6.
[45] Assi LN et al. Investigation of early compressive strength of fly ash-based geopolymer concrete. Constr Build Mater 2016;112:807–15.
[46] Shaikh F, Vimonsatit V. Compressive strength of fly-ash-based geopolymer concrete at elevated temperatures. Fire Mater 2015;39(2):174–88.
[47] Satpute S, Shirasath M, Hake S. Investigation of alkaline activators for fly ash-based geopolymer concrete. Int J Advance Res Innovative Ideas Educ (IJARIIE), ISSN 2016:2395–4396.
[48] Sumajouw M, Rangan BV. Low-calcium fly ash-based geopolymer concrete: reinforced beams and columns. 2006.
[49] Srinivasan S, Karthik A, Nagan D. An investigation on flexural behaviour of glass fibre reinforced geopolymer concrete beams. Int J Eng Sci Res Technol 2014;3(4):1963–8.
[50] Kumar S, P. J, Ravindra PM, Rajendra S. Flexural behaviour of fly ash based reinforced geopolymer concrete beams. Int J Struct Civil Eng Res 2014;3(3).
[51] Patankar SV, Jamkar SS, Ghugal YM. Effect of water-to-geopolymer binder ratio on the production of fly ash based geopolymer concrete. Int J Adv Technol Civ Eng 2013;2(1):79–83.
[52] Patankar SV, Ghugal YM, Jamkar SS. Mix design of fly ash based geopolymer concrete. In: Advances in Structural Engineering. Springer; 2015. p. 1619–34.
[53] Albitar M et al. Assessing behaviour of fresh and hardened geopolymer concrete mixed with class-F fly ash. KSCE J Civ Eng 2015;19(5):1445–55.
[54] Ishak S et al. Performance of fly ash geopolymer concrete incorporating bamboo ash at elevated temperature. Materials 2019;12(20):3404.
[55] Nuruddin MF, Demie S, Shafiq N. Effect of mix composition on workability and compressive strength of self-compacting geopolymer concrete. Can J Civ Eng 2011;38(11):1196–203.
[56] Lavanya G, Jegan J. Evaluation of relationship between split tensile strength and compressive strength for geopolymer concrete of varying grades and molarity. Int J Appl Eng Res 2015;10(15):35523–7.
[57] Raijiwala D, Patil H. Geopolymer concrete a green concrete. In: 2010 2nd international conference on Chemical, Biological and Environmental Engineering. IEEE, 2010.
[58] Hsu S, Chi M, Huang R. Effect of fineness and replacement ratio of ground fly ash on properties of blended cement mortar. Constr Build Mater 2018;176:250–8.
[59] Gholampour A, Gandomi AH, Ozbakkaloglu T. New formulations for mechanical properties of recycled aggregate concrete using gene expression programming. Constr Build Mater 2017;130:122–45.
[60] Lim JC, Karakus M, Ozbakkaloglu T. Evaluation of ultimate conditions of FRP-confined concrete columns using genetic programming. Comput Struct 2016;162:28–37.

[61] Perera R, Arteaga A, De Diego A. Artificial intelligence techniques for prediction of the capacity of RC beams strengthened in shear with external FRP reinforcement. Compos Struct 2010;92(5):1169–75.
[62] Perera R et al. Application of artificial intelligence techniques to predict the performance of RC beams shear strengthened with NSM FRP rods. Formulation of design equations. Compos B Eng 2014;66:162–73.
[63] Sadrmomtazi A, Sobhani J, Mirgozar M. Modeling compressive strength of EPS lightweight concrete using regression, neural network and ANFIS. Constr Build Mater 2013;42:205–16.
[64] Baykasoğlu A et al. Prediction of compressive and tensile strength of limestone via genetic programming. Expert Syst Appl 2008;35(1–2):111–23.
[65] Aval SB, Ketabdari H, Gharebaghi SA. Estimating shear strength of short rectangular reinforced concrete columns using nonlinear regression and gene expression programming. Structures. Elsevier; 2017.
[66] Mansouri I et al. Evaluation of peak and residual conditions of actively confined concrete using neuro-fuzzy and neural computing techniques. Neural Comput Appl 2018;29(3):873–88.
[67] Mansouri I et al. Predicting behavior of FRP-confined concrete using neuro fuzzy, neural network, multivariate adaptive regression splines and M5 model tree techniques. Mater Struct 2016;49(10):4319–34.
[68] Jalal M et al. Application of genetic programming (GP) and ANFIS for strength enhancement modeling of CFRP-retrofitted concrete cylinders. Neural Comput Appl 2013;23(2):455–70.
[69] Mashhadban H, Kutanaei SS, Sayarinejad MA. Prediction and modeling of mechanical properties in fiber reinforced self-compacting concrete using particle swarm optimization algorithm and artificial neural network. Constr Build Mater 2016;119:277–87.
[70] Dantas ATA, Leite MB, de Jesus Nagahama K. Prediction of compressive strength of concrete containing construction and demolition waste using artificial neural networks. Constr Build Mater 2013;38:717–22.
[71] Eskandari-Naddaf H, Kazemi R. ANN prediction of cement mortar compressive strength, influence of cement strength class. Constr Build Mater 2017;138:1–11.
[72] Sebaaly H, Varma S, Maina JW. Optimizing asphalt mix design process using artificial neural network and genetic algorithm. Constr Build Mater 2018;168:660–70.
[73] Velay-Lizancos M et al. Analytical and genetic programming model of compressive strength of eco concretes by NDT according to curing temperature. Constr Build Mater 2017;144:195–206.
[74] González-Taboada I et al. Prediction of the mechanical properties of structural recycled concrete using multivariable regression and genetic programming. Constr Build Mater 2016;106:480–99.
[75] Sadowski Ł et al. Hybrid ultrasonic-neural prediction of the compressive strength of environmentally friendly concrete screeds with high volume of waste quartz mineral dust. J Cleaner Prod 2019;212:727–40.
[76] Xie Q, Ni J-Q, Su Z. A prediction model of ammonia emission from a fattening pig room based on the indoor concentration using adaptive neuro fuzzy inference system. J Hazard Mater 2017;325:301–9.
[77] Zhu X, Wang X, Ok YS. The application of machine learning methods for prediction of metal sorption onto biochars. J Hazard Mater 2019;378:120727.
[78] Li Z et al. Polymorphisms of CHRNA5-CHRNA3-CHRNB4 Gene cluster and NSCLC risk in Chinese population. Transl Oncol 2012;5(6):448.
[79] Park S et al. Predicting PM10 concentration in Seoul metropolitan subway stations using artificial neural network (ANN). J Hazard Mater 2018;341:75–82.
[80] Getahun MA, Shitote SM, Gariy ZCA. Artificial neural network based modelling approach for strength prediction of concrete incorporating agricultural and construction wastes. Constr Build Mater 2018;190:517–25.
[81] Behnood A, Golafshani EM. Predicting the compressive strength of silica fume concrete using hybrid artificial neural network with multi-objective grey wolves. J Cleaner Prod 2018;202:54–64.
[82] Liu Q-F et al. Prediction of chloride diffusivity in concrete using artificial neural network: Modelling and performance evaluation. Constr Build Mater 2020:121082.
[83] Sudin R, Swamy N. Bamboo and wood fibre cement composites for sustainable infrastructure regeneration. J Mater Sci 2006;41(21):6917–24.
[84] Azim I et al. Semi-analytical model for compressive arch action capacity of RC frame structures. Structures. Elsevier; 2020.
[85] Gandomi AH et al. Novel approach to strength modeling of concrete under triaxial compression. J Mater Civ Eng 2012;24(9):1132–43.
[86] Gandomi AH, Yun GJ, Alavi AH. An evolutionary approach for modeling of shear strength of RC deep beams. Mater Struct 2013;46(12):2109–19.
[87] Ferreira C. Gene expression programming: mathematical modeling by an artificial intelligence. vol. 21. Springer, 2006.
[88] Azim I et al. Prediction model for compressive arch action capacity of RC frame structures under column removal scenario using gene expression programming. Structures. Elsevier; 2020.
[89] Javed MF et al. New prediction model for the ultimate axial capacity of concrete-filled steel tubes: an evolutionary approach. Crystals 2020;10(9):741.
[90] Mahdinia S, Eskandari-Naddaf H, Shadnia R. Effect of cement strength class on the prediction of compressive strength of cement mortar using GEP method. Constr Build Mater 2019;198:27–41.
[91] Azimi-Pour M, Eskandari-Naddaf H. ANN and GEP prediction for simultaneous effect of nano and micro silica on the compressive and flexural strength of cement mortar. Constr Build Mater 2018;189:978–92.
[92] Özcan F. Gene expression programming based formulations for splitting tensile strength of concrete. Constr Build Mater 2012;26(1):404–10.
[93] Jafari S, Mahini SS. Lightweight concrete design using gene expression programing. Constr Build Mater 2017;139:93–100.
[94] Ozbay E, Gesoglu M, Güneyisi E. Empirical modeling of fresh and hardened properties of self-compacting concretes by genetic programming. Constr Build Mater 2008;22(8):1831–40.
[95] Tanyildizi H, Çevik A. Modeling mechanical performance of lightweight concrete containing silica fume exposed to high temperature using genetic programming. Constr Build Mater 2010;24(12):2612–8.
[96] Sonebi M, Cevik A. Genetic programming based formulation for fresh and hardened properties of self-compacting concrete containing pulverised fuel ash. Constr Build Mater 2009;23(7):2614–22.
[97] Sarıdemir M. Genetic programming approach for prediction of compressive strength of concretes containing rice husk ash. Constr Build Mater 2010;24(10):1911–9.
[98] Oltean M, Dumitrescu D. Multi expression programming. J Genetic Programm Evolvable Machines, Kluwer, Second Tour of Review 2002.
[99] Arabshahi A, Gharaei-Moghaddam N, Tavakkolizadeh M. Development of applicable design models for concrete columns confined with aramid fiber reinforced polymer using Multi-Expression Programming. Structures. Elsevier; 2020.
[100] Alavi AH et al. Multi expression programming: a new approach to formulation of soil classification. Eng Comput 2010;26(2):111–8.
[101] Sharifi S, Abrishami S, Gandomi AH. Consolidation assessment using multi expression programming. Appl Soft Comput 2020;86:105842.
[102] Gandomi AH et al. New design equations for elastic modulus of concrete using multi expression programming. J Civil Eng Manage 2015;21(6):761–74.
[103] Koza, JR, Koza JR. Genetic programming: on the programming of computers by means of natural selection. vol. 1. MIT Press, 1992.
[104] Ali Khan M et al. Application of gene expression programming (GEP) for the prediction of compressive strength of geopolymer concrete. Materials 2021;14(5):1106.
[105] Shah MI, Javed MF, Abunama T. Proposed formulation of surface water quality and modelling using gene expression, machine learning, and regression techniques. Environ Sci Pollut Res 2020.
[106] Khan MA et al. Compressive strength of fly-ash-based geopolymer concrete by gene expression programming and random forest. Adv Civil Eng 2021;2021:6618407.
[107] Oltean M, Grosan C. A comparison of several linear genetic programming techniques. Complex Syst 2003;14(4):285–314.
[108] Hamad AJ. Size and shape effect of specimen on the compressive strength of HPLWFC reinforced with glass fibres. J King Saud Univ-Eng Sci 2017;29(4):373–80.
[109] Gandomi AH, Roke DA. Assessment of artificial neural network and genetic programming as predictive tools. Adv Eng Softw 2015;88:63–72.
[110] Mousavi S et al. A data mining approach to compressive strength of CFRP-confined concrete cylinders. Struct Eng Mech 2010;36(6):759.
[111] Babanajad SK, Gandomi AH, Alavi AH. New prediction models for concrete ultimate strength under true-triaxial stress states: An evolutionary approach. Adv Eng Softw 2017;110:55–68.
[112] Gandomi AH et al. Nonlinear genetic-based models for prediction of flow number of asphalt mixtures. J Mater Civ Eng 2011;23(3):248–63.
[113] Ahmad A et al. Prediction of compressive strength of fly ash based concrete using individual and ensemble algorithm. Materials 2021;14(4):794.
[114] Tkaczewska E. Effect of the superplasticizer type on the properties of the fly ash blended cement. Constr Build Mater 2014;70:388–93.

Dr. M. Ijaz Khan is working as a Assistant Professor in the Department of mathematics Riphah International University, Faisalabad Campus, Faisalabad. He is working mainly in the field of Newtonian, non-Newtonian fluid mechanics, Porous Media, Heat and mass transfer, stretching sheet, stretching cylinders, curved surfaces etc.